Journal of the European Ceramic Society 16 (1996) 833–841

0955-2219(95)00211-1
0955-2219/96/$15.00 +.00

Morphology of Lanthanum Carbonate Particles Prepared by Homogeneous Precipitation

Martin L. Panchula & Mufit Akinc

Department of Materials Science & Engineering, Iowa State University, Ames, Iowa 50011, USA

(Received 10 July 1995; revised version received 22 November 1995; accepted 29 November 1995)

Abstract

The synthesis of lanthanide oxide precursor particles through urea decomposition has received considerable attention over the past few years. It was previously reported by several different workers that the synthesis of spherical, monodispersed light lanthanide ceramic precursor particles was consideably more difficult than the precipitation of spherical particles from the heavy lanthanide elements. These difficulties have been overcome to a large extent by proper choice of processing conditions. This paper describes the synthesis conditions for which dispersed spherical particles and plates may be formed of lanthanum, the lightest of the lanthanide elements. The experimental conditions for the synthesis of these particles is given in the form of morphological diagrams and the chemistry and yield of the process is also reported. The process was also analyzed as a function of time in order to observe the supersaturation and growth regimes. The effect of calcining on the morphology of the particles is also discussed.

1 Introduction

It was previously reported by Akinc and Sordelet[1] that lanthanum, cerium, and neodymium powders precipitated as crystalline basic carbonate particles when urea was used as the precipitating agent. Yttrium, on the other hand, and the heavy rare earths,[2] defined in this paper as those heavier than gadolinium, precipitated as spherical, amorphous particles under similar conditions. Recently, it was shown that the light lanthanides can be precipitated as spherical monodispersed particles through the proper choice of initial conditions[3–6] and by the proper choice of supporting anions.[7] These reports demonstrate the sensitivity of particle morphology to subtle variations in experimental conditions.

The growth of monosized, spherical particles has been explained by two mechanisms. The first mechanism is that of spontaneous accumulation of polymeric species and subsequent particle sharpening as a result of radius dependent particle growth during aging. Formation of latex particles was shown to follow this mechanism. The second mechanism is the aggregation of nuclei to form spherical particles. Bogush and Zukoski[8,9] claimed that formation of silica from tetra ethyl ortho silicate (TEOS) follows the aggregation mechanism. Visible proof of the aggregation mechanism has been reported by Celikkaya and Akinc[10] in the precipitation of zinc sulfide particles from thioacetamide solutions where spherical polycrystalline particles were formed. Nanocrystalline aggregates of sphalerite crystallites were observed in SEM and TEM micrographs.

The accepted precipitation mechanism for well developed euhedral particles is based upon the accumulation of ionic species on the surface of nuclei. Preferential growth planes, as determined by surface energy and kinetic restrictions, will then result in euhedral particle (particles with well defined shapes, faces) formation. A number of colloids were precipitated with either spherical or euhedral morphology with relatively subtle changes in experimental conditions such as kinetics of precipitation. It appears that a third mechanism in the formation of spherical particles is operative such that a fast accumulation of ions will also yield spherical particles.

The present work extends the work of Akinc and Sordelet[1] on the synthesis of crystalline euhedral light lanthanides to precipitate spherical monodispersed lanthanum carbonate particles by homogeneous precipitation using urea as the precipitating agent. Morphological diagrams and process yields for a wide range of initial conditions are reported. Additionally, the influence of calcining on the particle morphology and chemistry is also examined.

2 Experimental Procedure

2.1 Materials

The lanthanum stock solution was prepared by dissolving 99·9% pure La_2O_3 (Molycorp) in nitric

acid (Malinckrodt). The solution was then diluted to approximately 0·5 M with respect to La^{3+} ion and filtered through a 0·22 μm Teflon® membrane (Micron Separations, Inc). It is particularly important for homogeneous precipitation studies that no foreign particles which might act as seed crystals enter into the reaction vessel. For this reason, the lanthanum solution was acidified through the addition of excess nitric acid and heated to remove what appeared to be spontaneous lanthanum carbonate formation within the storage container. The urea stock solution, with a concentration of 6·75 M, was prepared by dissolving the appropriate amount of urea in deionized water and filtering through a 0·2 μm Teflon® membrane. This solution was then kept refrigerated to prevent decomposition of urea during storage.

2.2 Powder synthesis

Appropriate amounts of deionized water and lanthanum stock solution were combined in a 400 cm^3 beaker. The pH of this solution was then adjusted at room temperature by adding ammonium hydroxide or nitric acid. The pH of the solution was continuously recorded using a temperature compensated pH meter (Fisher Accumet 810 MP). The beaker was then covered and placed in a circulated hot water bath which was set at 95°C. When the solution reached 95°C, the appropriate amount of the urea stock solution was added to bring the solution up to 250 cm^3 and the beaker resealed and placed in the water bath. The solution was aged for 90 min from the time at which visible nucleation occurred. At the end of the aging period, the beaker was placed in a cold water bath to quench the reaction. Suspension was then centrifuged until a clear supernatant was obtained. The centrifugation was repeated twice with water and once with acetone. After the acetone wash, the precipitate was dried in air at 85°C for overnight.

2.3 Powder characterization

The powder morphology was examined using a scanning electron microscope (JEOL JSM 6100). Thermal decomposition of precursor particles was studied by a thermogravimetric analyzer (Seiko TGA/DTA 300). Approximately 10–40 milligrams of the sample, was heated to 900°C at a rate of 3° min^{-1} in a dry air atmosphere with a flow rate of 100 cm^3 min^{-1}. Crystal structure of the powders was studied by X-ray powder diffraction unit (Scintag XDS 2000). The powder diffraction patterns were compared against JCPDS standards using the Diffraction Management System 2000 software package.

3 Results and Discussion

3.1 Precipitation process

Homogeneous precipitation by urea can be considered as self regulating due to equilibria established between carbonic acid and ammonia which are released by urea decomposition. Dissociation constants of carbonic acid and ammonia are comparable that in the absence of strong acids or bases, the concentrations of OH^- and $CO_3^=$ ions are maintained within a narrow range during precipitation. However, by changing the initial pH of the solution one can affect the quantity of urea which will decompose before supersaturation is achieved. In this way, the chemistry of the solution, the $[OH^-]/[CO_3^=]$ ratio for instance, can be adjusted.

Figure 1 shows the variation of pH with time for solutions with a different initial pH. As the plots clearly depict, the pH of the solutions is essentially identical after the initial 5 min. The nucleation, growth, and cation exhaustion can all be seen by measuring the pH of the system during precipitation. This can be seen most easily at low cation concentrations and relatively high pH solutions. Maxima observed in the early stages represent the critical supersaturation and onset of nucleation. The pH decrease with particle growth is expected as the precipitation of any carbonate will remove $CO_3^=$ ions from the solution, shifting the $HCO_3^- = CO_3^= + H^+$ equilibrium to right and releasing H^+ ions, thus decreasing the pH of the solution. Similarly, if the precipitate involves hydroxides, removing OH^- ions from the medium results in a decrease in pH. Once the cation is exhausted, however, and if there is sufficient urea remaining in solution, the pH will start to increase again signalling the end of precipitation. The differences seen between the low and high initial pH solutions are due to the time it takes for the low initial pH solutions to decompose sufficient urea

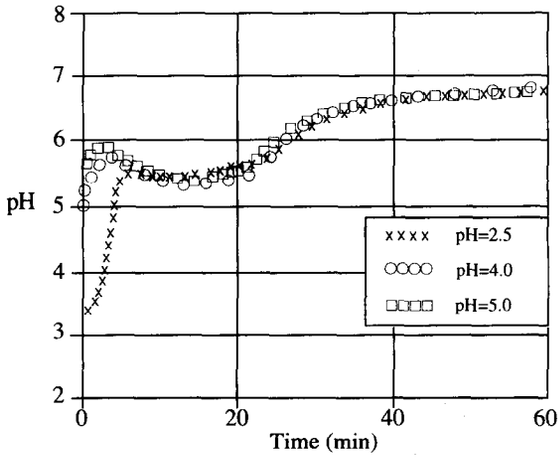

Fig. 1. pH–time curve for lanthanum precipitation from 0·005 M lanthanum solutions of various initial pH (prior to urea addition) and with an initial urea content of 0·054 M and a reaction temperature of 95°C.

to increase the pH to the point where precipitation can occur. This additional time allows more urea to decompose prior to precipitation and this will affect the total carbonate content which will, in turn, affect the ionic strength of the solution. The additional charged species will effectively buffer the solution making the supersaturation region more difficult to detect.

3.2 Morphology

As stated earlier, amorphous spherical particles should be the result of the addition of polymeric, or at least complexing, species to nuclei. On the other hand, the growth of euhedral particles is caused by the addition of ions to the surface of a nucleus with crystalline faceting occurring due to fast and slow growth directions. Lanthanum carbonate particles have been precipitated in this study with both spherical and 'square planar' morphologies (Fig. 2). The morphological diagrams show the effects of the various initial conditions on the resulting morphologies as depicted in Table 1.

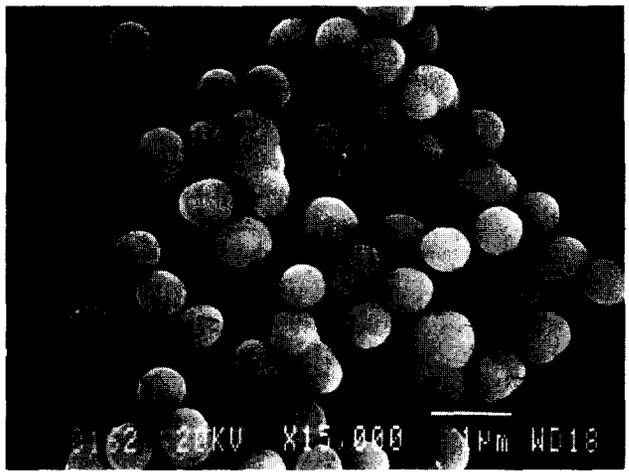

(a)

(b)

Fig. 2. Micrographs of the sperical and square planer morphologies as described above. Notice the spherical particles which have grown on the faces of the square planar precipitates.

Table 1. Plot of particle morphology map as a function of lanthanum ion concentration and initial pH. Reaction temperature T = 95°C. S = Spherical, E = Euhedral, SP = Square planar

Initial pH	*Urea*	*Cation concentration, moles/l*			
		0·005	*0·025*	*0·045*	*0·65*
5·0	0·54	S	E, S	E	—
4·0	0·54	S	E, S	E	—
2·5	0·54	S, E	E, S	E, S	—
1·0	0·54	E	E	E	—
5·0	0·27	S, E	S, E	E	—
4·0	0·27	S, E	SP, S	SP, S	SP, S
2·5	0·27	S, E	SP, E, S	SP, S	SP, S, E
1·0	0·27	E	E		

There are essentially two interesting morphologies created in this system; spheres (S) and square planar (SP) particles. The spheres generally have a smooth surface with few or no surface features present. This suggests an amorphous growth process.

The square planar morphology is perhaps the more interesting. Generally they are 3 μm on a side yet only 0·2 μm thick. In fact, they are translucent to the 20 keV electron beam when viewed perpendicularly to the flat face. A high percentage of the square planar particles have what appear to be spherical particles growing on their faces. Presumably, these particles nucleated and grew after the square planar particles were formed.

The other morphologies mentioned in Table 1 are highly agglomerated with a wide variety of particle morphologies as one would expect from intermixed nucleation and growth processes. The particles described as euhedral are large (> 5 μm) particles with characteristic features exhibited by crystalline materials such as sharp angles and edges.

3.3 Yield

The yield of this process, defined as percentage of initial cation precipitated, is primarily dependent upon the amount of urea decomposed. The amount of urea decomposed at time t is given by the difference between the initial urea concentration, U_0, and urea concentration, U_t, at time t:

$$U_d = U_0 - U_t \tag{1}$$

Where U_d is the concentration of urea decomposed up to time, t.

$$U_t = U_o\,[\exp(-kt)] \tag{2}$$

Substituting this back in eqn (1) results in

$$U_d = U_o\,[1-\exp(-kt)] \tag{3}$$

On the other hand, rate of urea decomposition is given by:[1]

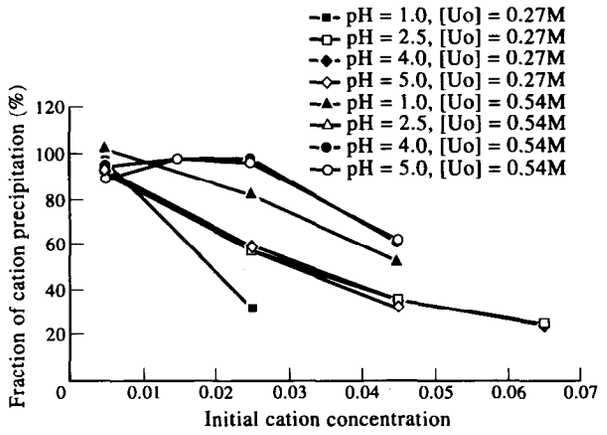

Fig. 3. Yield of the precipitation runs as a function of initial conditions. The reaction temperature was held constant at 95°C.

$$k = (4{\cdot}57 \times 10^{10}\ \text{min}^{-1}) \exp\left(\frac{-96{\cdot}127\ \text{kJ/mole}}{RT}\right) \quad (4)$$

Where R is the gas constant and T is the temperature in degrees Kelvin.

Obviously, both temperature and initial urea concentration can play a large role in the amount of urea decomposed as a function of time. In a related study we showed how temperature, and hence the decomposition rate, affected the yield of neodymium and europium samples.[3] In this paper we show how initial urea concentration and pH affect the yield. As can be seen in Fig. 3, there are four sets of curves. The curves for pH of 2·5, 4, and 5 are grouped together but are separated depending on the concentration of initial urea. The pH=1 samples generally have lower yields than the other pH levels, though this too is dependent on initial urea concentration. The apparent drop in yield at very low concentrations is due to the fact that small sample losses during sample transfer and centrifugation correspond to a larger fraction of the total cations in the solution. The separate curves for the pH=1 condition can only be explained by the fact that much longer times were necessary for the urea to decompose and produce sufficient quantities of hydroxide ions to raise the pH to the point where precipitation could occur. Therefore, initial urea concentration, $[U_0]$, was effectively reduced prior to precipitation. Low initial pH also results in higher $[CO_3^{=}]/[OH^-]$ ratio during nucleation and growth which will likely alter the chemical composition and morphology of the particles produced.

3.4 Thermal decomposition

The thermal decomposition of the precipitated powder depends upon the chemistry and morphology of the powders. For example, Fig. 4 shows the weight loss on heating of the monodispersed spherical particles (upper curve) and of the square planar precipitates, (lower curve). One subtle difference between the two curves is that the spherical particles appear to have slightly smoother weight loss up to the formation of the dioxycarbonate compared to the square planar particles. This is believed to be due to the degree of crystallinity of the samples and not to any large differences in particle chemistry. Spherical particles also exhibit a small weight loss below 100°C, perhaps due to evolution of adsorbed water. Previous experiences with the light lanthanides precipitated and dried in the same manner as used here have given approximately two waters of hydration for the simple carbonate precipitate. The calculated weight loss data presented in Table 2 are based upon the assumption that the precipitated particles were in the form of $La_2(CO_3)_3 \cdot 1{\cdot}4H_2O$. The experimental values shown in the table are averaged from five TGA runs on powders precipitated under different conditions. The difference between the high and low experimental values at

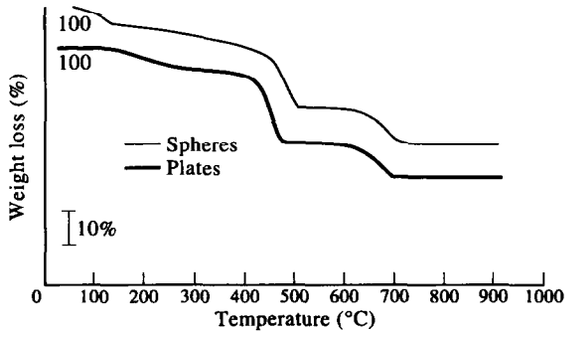

Fig. 4. Weight loss on heating of spherical (upper TGA curve) and square planar (lower TGA curve) lanthanum particles on heating in zero air.

Table 2. Comparison of experimental and calculated weight loss values for precipitated lanthanum carbonate particles with an approximate composition of $La_2(CO_3)_3 \cdot 1{\cdot}4H_2O$

Resultant particle chemistry	*Reaction*	*Calculated weight loss*	*Experimental weight loss*
Dehydrated carbonate	$La_2(CO_3)_3 \cdot 1{\cdot}4H_2O \rightarrow La_2(CO_3)_3$	7·3%	4·9% 50–300°C
Dioxycarbonate	$La_2(CO_3)_3 \rightarrow La_2O_2CO_3$	19·2%	19·8% 423°C
Oxide	$La_2O_2CO_3 \rightarrow La_2O_3$	11·9%	11·7% 630°C

each weight loss step was less than 3%. In Table 2 the sample weight loss from the dehydrated carbonate to the dioxycarbonate and the dioxycarbonate to the oxide are identical within the experimental error.

3.5 X-ray analysis

The crystal structure of the spherical and square planar particles was analyzed by X-ray powder diffraction. The spherical particles gave an amorphous pattern as expected. The square planar particles, however, gave relatively weak diffraction patterns making phase identification difficult (Fig. 5). In addition, because of the two-dimensional nature of the particle growth habit, the relative peak intensities were probably greatly biased. Based upon TGA and chemical analysis, it was expected that the particles would give the lanthanite ($La_2(CO_3)_38H_2O$) diffraction pattern. It appears that the lanthanite structure was lost in favor of an amorphous structure upon drying at 85°C leaving only the minor phase, the monoxycarbonate structure ($La_2O(CO_3)_2xH_2O$) as the crystalline phase. There is some evidence to support the idea that the lanthanite structure does not completely collapse, in that some residual lanthanite peaks including the one at $2\theta=18{\cdot}4°$ survived the drying process. This peak corresponds to (020) plane in the orthorhombic structure. The intensity of this peak varies from sample to sample, possibly the result of different drying conditions. The crystal is a layered structure with lanthanum and carbonate ions forming planes which are separated by planes of water molecules.[11,12] It is possible that certain directions in this highly hydrated crystal structure would collapse first leaving other planes relatively untouched. The observed peak does not correspond to any other lanthanum phase in the JCPDS files. The crystalline phase of anhydrous lanthanum carbonate can only be produced from the lanthanite phase after drying the sample in a vacuum and then heating to 430°C in a 100 kPa CO_2 atmosphere.[13]

The coefficient x for the number of crystalline waters in the monoxycarbonate formula can vary between 1 and 2, just as the TGA analysis suggested. It has been reported by previous workers[14] that drying the eight hydrate lanthanite phase at less than 100°C or placing it in a vacuum results in a primarily amorphous phase due to dehydration. This effect is shown in Fig. 6. The room temperature dried samples exhibit distinct peaks of $La_2(CO_3)_38H_2O$. There are additional, albeit much weaker peaks due to partially hydrated monoxycarbonate, ($La_2O(CO_3)_2xH_2O$). After drying at 85°C the major crystalline phase appears to be the partially hydrated monoxycarbonate, $La_2O(CO_3)_2xH_2O$. The precipitate appears to be mostly amorphous with a small fraction of crystalline phase (monoxycarbonate). Since the particles are small and exhibit large dimensional anisotropy, the peak intensities are questionable. The phase which was assigned as the monoxycarbonate might also be identified as the basic carbonate phase. In fact, chemically it makes no difference whether the particles are monoxycarbonate with one water of hydration, ($La_2O(CO_3)_2H_2O$) or basic carbonate with no waters of hydration, ($2LaOHCO_3$). The basic

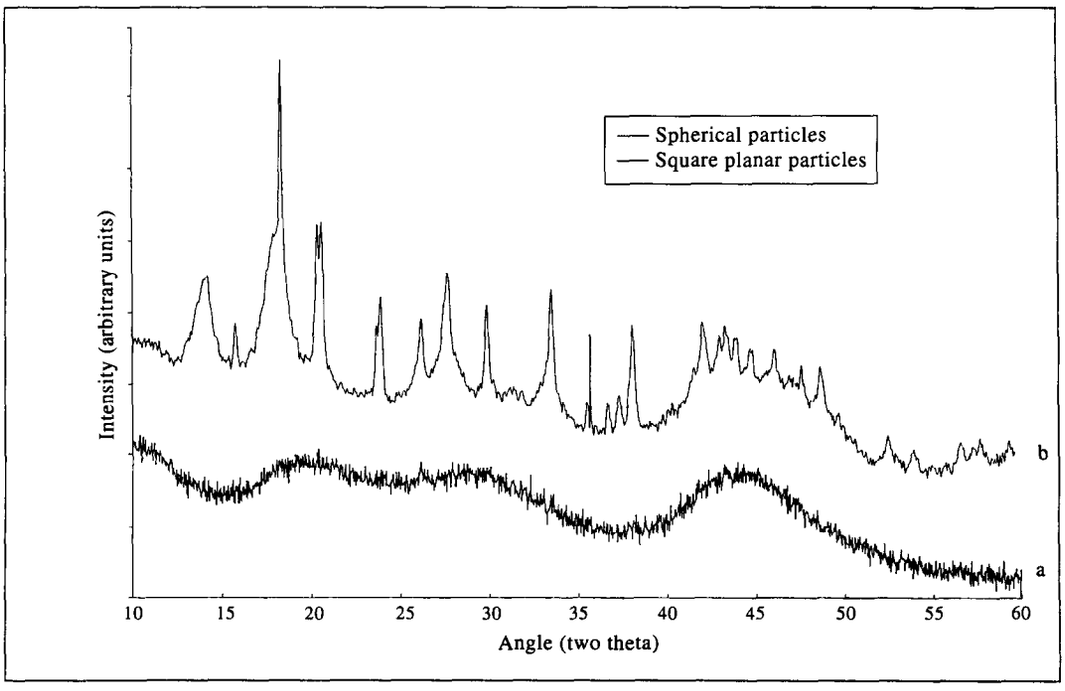

Fig. 5. X-ray diffraction pattern of (a) spherical, (b) square planar particles.

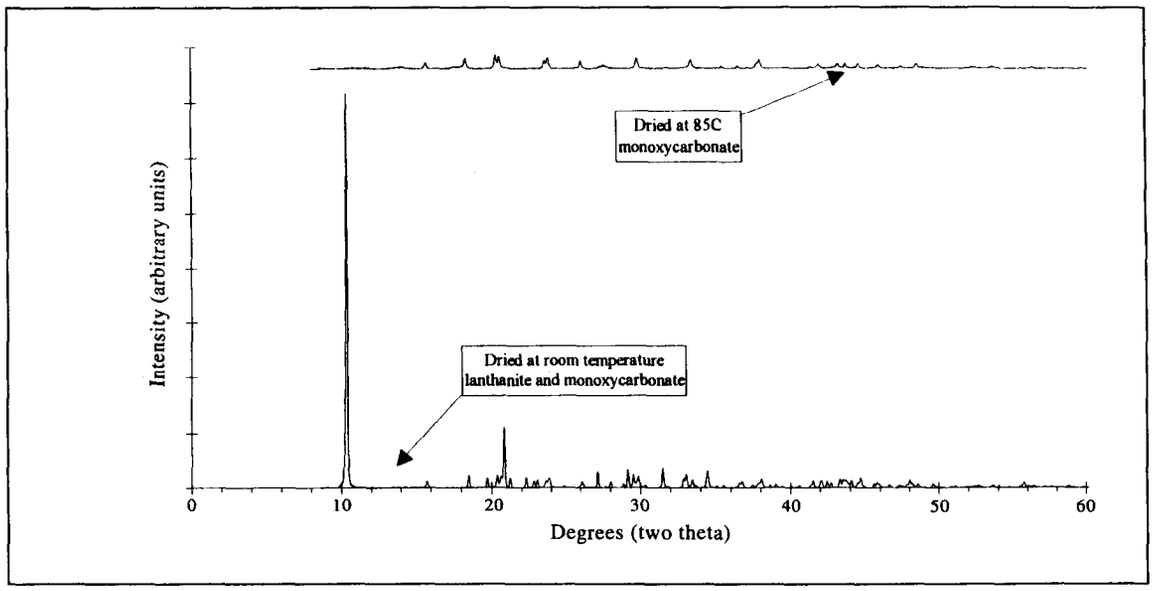

Fig. 6. Effect of drying conditions on crystalline structure as observed through X-ray diffraction

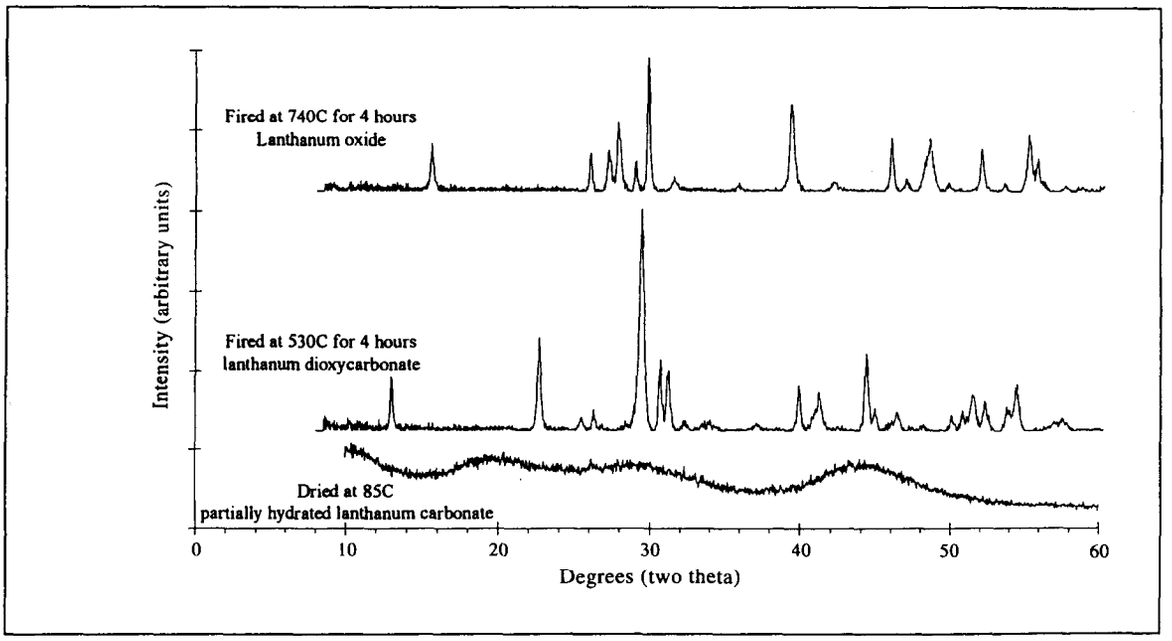

Fig. 7. Effect of firing on crystalline phases and X-ray peak intensity of spherical particles.

carbonate was the only phase observed in heavy lanthanides synthesized by a similar procedure, but without further evidence the structure of this phase is ambigious.

The X-ray diffraction patterns of the powders at 530 and 740°C are shown in Figs 7 and 8. Figure 7 shows that as-precipitated amorphous spherical particles have decomposed and ordered themselves into a dioxycarbonate structure as was predicted by thermogravimetric analysis. The square planar particles show the same trend, with the dioxycarbonate being the stable form at 530°C and the oxide the stable form at 740°C.

3.6 Effect of heating on particle morphology

The influence of calcining on the particle morphology was investigated, heating the spherical and square planar particles in air to 530 or 740°C for 4 h. Both samples were converted to oxide at 740°C. The particle morphology as a function of heat treatment is shown in Figs 9 and 10. The spherical particles became slightly faceted after being heated to 530°C. At 740°C, the particles became crystalline. Monodispersity and overall size and shape of the precursor particles are retained (Fig. 9). The square planar particles showed only subtle changes on being heated to 530°C. The surfaces of the particles became rough

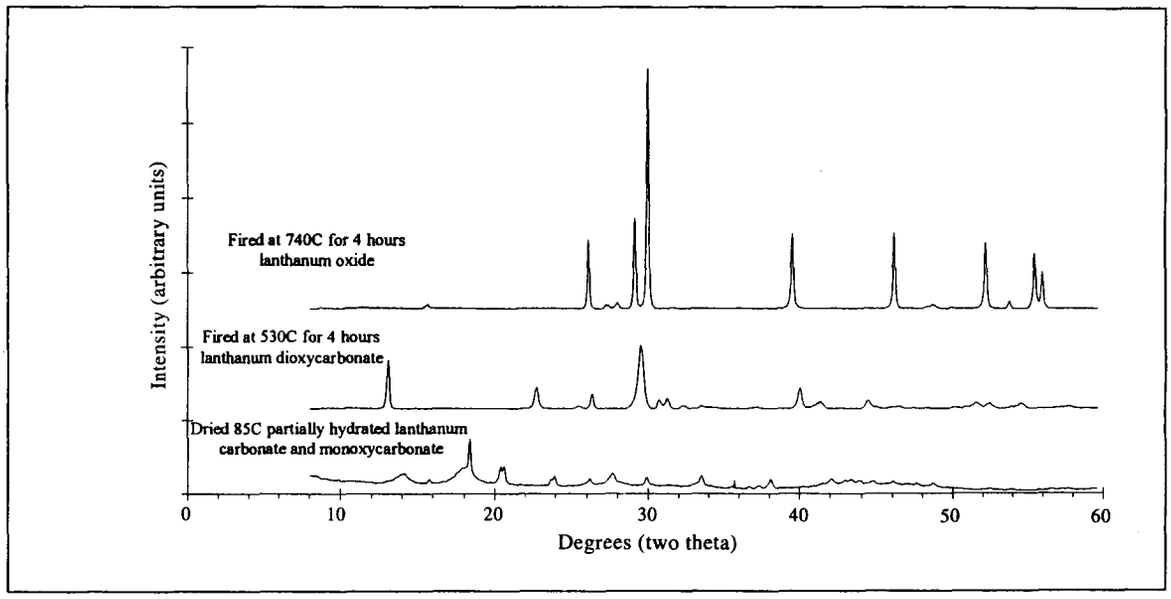

Fig. 8. Effect of firing on crystalline phases and X-ray peak intensity of square planar particles.

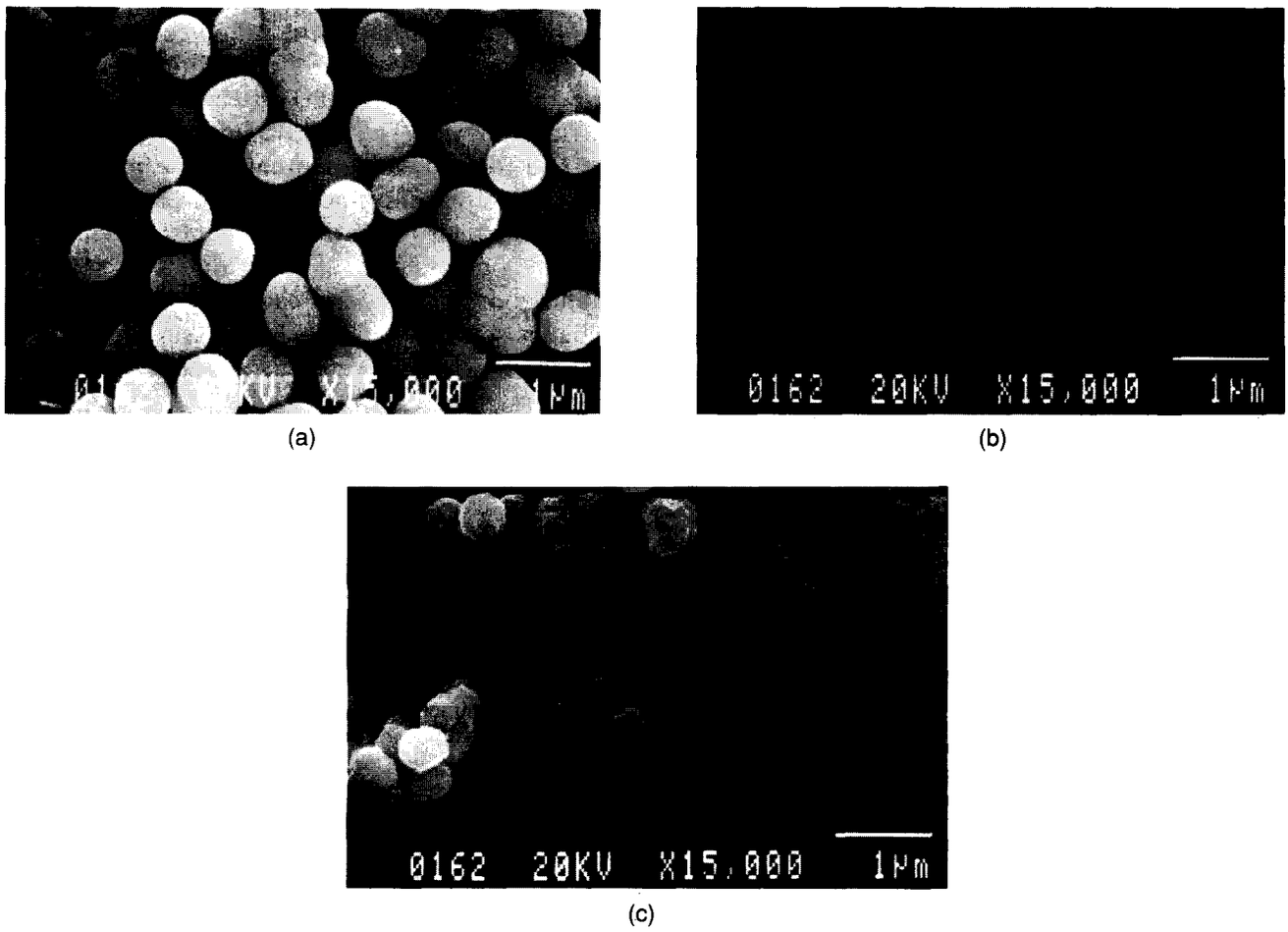

Fig. 9. Effect of heating on spherical lanthanum particle morphology: (a) original particles; (b) after heating to 530°C for 4 h, and (c) after heating to 740°C for 4 h.

and appear to indicate polycrystallinity. At 740°C, the changes are more obvious. The previously smooth surfaces now consist of smaller grains which are sintered together while maintaining the shape of the original plate. The spherical growths on the plates have gone through the same changes as the monodispersed particles shown in Fig. 9 with perhaps more sintering to the surface of the

(a)

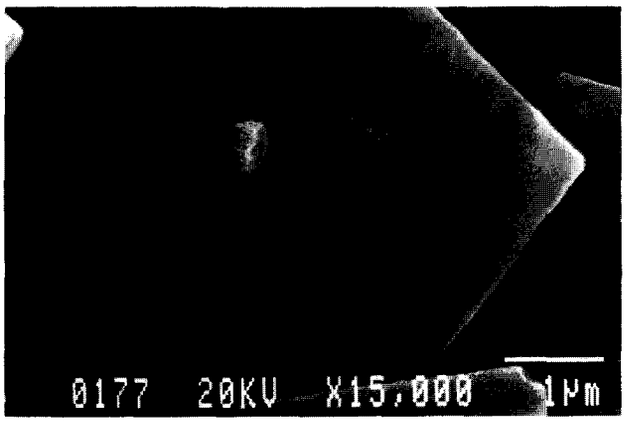

(b)

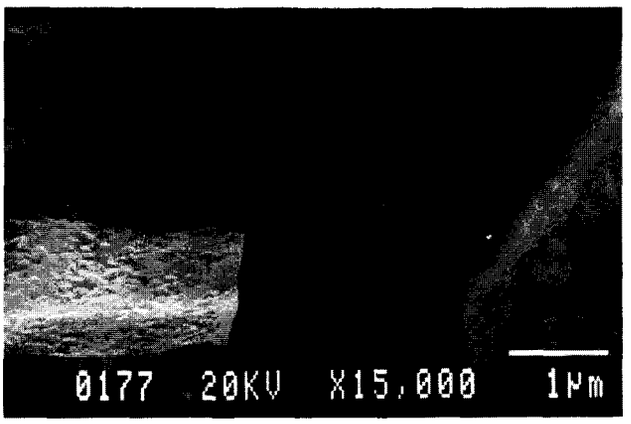

(c)

Fig. 10. Effect of heating on square planar particle morphology: (a) original particles; (b) after heating to 530°C for 4 h, and (c) after heating to 740°C for 4 h.

square planar particles due to the larger initial contact area.

4 Conclusion

Spherical and square planar lanthanum carbonate particles have been synthesized by homogeneous precipitation employing urea as the precipitating agent. It is apparent that the two growth mechanisms are quite different, yet can be achieved in very similar systems. This result underscores the importance of process and variable control when using homogeneous precipitation for the synthesis of ceramic powders. The cause of the different morphologies is derived from two requirements which have been met in different ways resulting in two distinctly different morphologies. The two requirements are the degree of supersaturation before nucleation and the growth rate. At very low cation concentrations and high urea concentrations the supersaturation is relatively large, resulting in a large burst of nuclei and very quick growth. This growth period would be relatively short, lasting only until the remaining cation is completely precipitated. This mechanism has resulted in spherical particles. On the other hand, higher cation concentrations form stable nuclei earlier in the process, thereby keeping the supersaturation level relatively low. Under these conditions a slow growth of the nuclei is expected. Such conditions would allow for formation of euhedral particles. A direct examination of the cation concentration as a function of time would offer great insights into the growth mechanisms of this system and has not been carried out yet. This study, however, provided a method for producing lanthanum carbonate particles of different morphologies and plausible explanation for their formation mechanisms. This study also demonstrated for the first time that spherical, submicron size particles can be synthesized from aqueous solutions at ambient pressures.

References

1. Akinc, M. & Sordelet, D., Preparation of Yttrium, Lanthanum, Cerium, and Neodymium Basic Carbonate Particles by Homogeneous Precipitation. *Advanced Ceramic Materials*, **2** (3A) (1987) 232–8.
2. Akinc, M., Sordelet, D. & Munson, M., Formation, Structure, and Decomposition of Lanthanide Basic Carbonates. *Advanced Ceramic Materials*, **3**(3) (1988) 211–16.
3. Panchula, M. & Akinc, M., Precipitation of Neodymium and Europium Ceramic Precursor Particles through Urea Decomposition. To be published.
4. Kang, Z. C., Li, T. Z. & Eyring, L., The Preparation of Hydroxycarbonate Colloidal Particles of Individual and Mixed Rare Earth Elements. *Journal of Alloys and Compounds*, **181** (1992) 477–82.
5. Chou, K., Lin, C., Hoh, Y. & Miao, Y., Effect of Hydrothermal Synthesis Conditions on the Morphology of Lanthanum Hydroxycarbonate Colloids. *Journal of the Chinese Institute of Chemical Engineering*, **22**(4) (1991) 241–6.
6. Chu, Xi, Chung, W. & Schmidt, L. D., Sintering of Sol–Gel–Prepared Submicrometer Particles Studied by Transmission Electron Microscopy. *Journal of the American Ceramic Society*, **76**(8) (1993) 2115–18.
7. Matijevic, E. & Hsu, W. P., Preparation and Properties of Monodispersed Colloidal Particles of Lanthanide Compounds I. Gadolinium, Europioum, Terbium, Samarium, and Cerium (III). *Journal of Colloid and Interface Science*, **118**(2) (1987) 506–23.

8. Bogush, G. H. & Zukoski, IV, C. F., Studies of the Kinetics of the Precipitation of Uniform Silica Particles through the Hydrolysis and Condensation of Silicon Alkoxides. *Journal of Colloid and Interface Science,* **142** (1) (1991) 1–18.
9. Bogush, G. H. & Zukoski, IV, C. F., Uniform Silica Particle Precipitation: An Aggregative Growth Model. *Journal of Colloid and Interface Science*, **142**(1) (1991) 19–34.
10. Celikkaya, A. & Akinc, M., Preparation and Mechanism of Formation of Spherical Submicrometer Zinc Sulfide Powders. *Journal of the American Ceramic Society*, **73**(8) (1990) 2360–5.
11. Shinn, D. B. & Eck, H. A., The Crystal Structure of Lanthanum Carbonate Octahydrate. *Inorganic Chemistry,* **7**(7) (1968) 1340–5.
12. Dal Negro, A., Rossi, G. & Tazzsoli, V., The Crystal Structure of Lanthanite. *American Minerologist,* **62** (1977) 142–6.
13. Leskela, M. & Niinisto, L., *Handbook on the Physics and Chemistry of Rare Earths*, ed. K. A. Gschneidner & L. Eyring, Chapter 56, Vol 8, North-Holland, New York, 1986.
14. Sawyer, J., Caro, P. & Eyring, L., Hydroxy-carbonates of the Lanthanide Elements, *Revue de Chimie Mineral*, **10** (1973) 93–104.